

# Confinement-Induced Floquet Engineering and Non-Abelian Geometric Phases in Driven Quantum Wire Qubits

O. C. Feulefack<sup>a</sup>, S. L. Dongmo Tedo<sup>b</sup>, J. E. Danga<sup>b,c,d</sup>, R.M. Keumo Tsiaze<sup>a,c,e</sup>, F. Melong<sup>f</sup>, C. Kenfack Sadem<sup>a,b,c</sup>, A. J. Fotue<sup>b</sup>, M. N. Hounkonnou<sup>a</sup>, L.C. Fai<sup>b,c</sup>

<sup>a</sup> International Chair in Mathematical Physics and Applications, (ICMPA-UNESCO Chair), University of Abomey-Calavi, 072 P O Box 50, Cotonou, Republic of Benin.

<sup>b</sup> Condensed Matter and Nanomaterials, Department of Physics, Faculty of Science, University of Dschang, P.O. Box 67, Dschang, Cameroon.

<sup>c</sup> Quantum Materials and Computing Group - QMaCG, P.O. Box 70 Bambili, Northwest Region, Cameroon.

<sup>d</sup> Instituteur principal de l'enseignement général, Délégation Régionale de l'Ouest, Délégation Départementale de la Menoua, Arrondissement de Nkong-Ni, Ecole Publique de Batsing la Chefferie, Bafou, Cameroun.

<sup>e</sup> Laboratory of Mechanics, Materials and Structures, Faculty of Science, University of Yaoundé I, P.O. Box 812, Yaoundé, Cameroon. and

<sup>f</sup> Mathematisches Institut der Universität Münster Einsteinstr. 62, 48149 Münster, Germany.\*

This work theoretically demonstrates that a spin qubit in a parabolic quantum wire driven by a bichromatic field exhibits a confinement-tunable synthetic gauge field, leading to novel Floquet topological phenomena. The study presents the underlying mechanism for topological protection of qubit states against time-periodic perturbations. The analysis reveals a confinement-induced topological Landau-Zener transition, marked by a shift from preserved symmetries to chiral interference patterns in Landau-Zener-Stückelberg-Majorana interferometry. Notably, the emergence of non-Abelian geometric phases under cyclic evolution in curved confinement and phase-parameter space is identified, enabling holonomic quantum computation. Additionally, the prediction of unconventional Floquet-Bloch oscillations in the quasi-energy and resonance transition probability spectra as a function of the biharmonic phase indicates exotic properties, including fractal spectra and fractional Floquet tunneling. These phenomena provide direct evidence of coherent transport in the synthetic dimension. Collectively, these findings position quantum wire materials as a versatile platform for Floquet engineering, topological quantum control, and fault-tolerant quantum information processing.

PACS numbers: 03.67.Lx, 73.21.Hb, 32.80.Xx, 42.50.Hz, 03.65.Vf

Keywords: Spin Qubit, Quantum Wire, LZSM Interferometry, Synthetic Gauge Field, Non-Abelian Phase, Floquet Theory.

## I. INTRODUCTION

The development of fault-tolerant quantum information processing has driven significant research into platforms that enable coherent control and protection of quantum states from decoherence. Semiconductor quantum wires, due to their high integrability and tunable electronic confinement, represent a promising architecture for hosting spin qubits [1–10]. Nevertheless, achieving quantum coherence alongside high-fidelity operations remains a major challenge.

---

\* edmonddanga1@yahoo.com, keumoroger@gmail.com, hounkonnou@yahoo.fr, corneliusfai@gmail.com

Floquet engineering, which involves controlling quantum systems through periodic driving, has become a prominent approach for generating novel non-equilibrium quantum phases with enhanced robustness [11–13]. Within this context, Landau-Zener-Stückelberg-Majorana (LZSM) interferometry is a critical technique for probing and manipulating driven qubits [14–16]. Recent advances indicate that stronger electronic confinement can improve the control of rapid quantum tunneling, thereby preserving spin states during LZSM interferometry transitions [17–20]. Although monochromatic drives have been extensively investigated [21, 22], biharmonic fields provide a broader control landscape and greater phase sensitivity [23, 24]. Prior research has addressed minimizing noise effects [25, 26] and exploring nonlinear qubit dynamics [27–29, 31, 32] to regulate topological photonic gap magnitudes across various field-induced energy spectra. However, the behavior of qubits under biharmonic fields remains insufficiently understood.

Recent advances in Floquet engineering have demonstrated the potential of driven systems to generate topological phases [33] and implement geometric quantum gates [34]. Time-periodic forcing has been utilized within Floquet engineering as a powerful method to control and modify quantum systems, exemplified by the discovery of novel out-of-equilibrium topological phases [35, 36]. Furthermore, these techniques have been proposed to enhance precision measurement in quantum metrology [37–39] and to advance holonomic quantum computing [40–42].

This study theoretically demonstrates that the interplay between tunable parabolic confinement  $\Omega$  and a biharmonic electromagnetic drive gives rise to phenomena beyond conventional LZSM interferometry. The analysis utilizes perturbation-resonant theory protocols [43–45] and a quasi-energy framework [46] to examine the influence of curved confinement and simultaneous biharmonic control fields on the system's energy spectrum and transition probabilities. Notably, a confinement-induced topological Landau-Zener (LZ) transition is identified, marked by a transition from preserved symmetries to chiral interference patterns in LZSM interferometry. The combined effects of curved confinement and biharmonic control facilitate the realization of topologically non-trivial geometrical qubits and photonic gaps, underscoring the significant impact of fractal spectra and fractional Floquet tunneling as direct signatures of coherent transport in synthetic dimensions. Furthermore, geometrical qubits exhibit resilience to certain types of noise, suggesting their suitability for fault-tolerant quantum computing [41, 47–49]. The central findings reveal the interdependence of tunable parabolic confinement  $\Omega$ , biharmonic electromagnetic drive, topological LZ transitions, unconventional Floquet-Bloch oscillations, and non-Abelian geometric phases, which collectively offer promising avenues for controlling unconventional quantum states and coherent transport through engineered lattices and interactions. The results indicate that variation in  $\Omega$  induces a topological LZ transition [50, 51] in the Floquet spectrum, fundamentally transforming interference patterns from symmetric to chiral. Additionally, cyclic evolution in the  $(\Omega, \theta)$  parameter space gives rise to non-Abelian geometric phases, enabling holonomic quantum computation. Oscillatory behavior in the quasi-energy and transition probability spectra as a function of  $\theta$  is predicted, analogous to Bloch oscillations in crystalline solids. Collectively, these findings position quantum wires as a robust platform for topological quantum control and fault-tolerant quantum information processing.

The structure of the paper is as follows. Section II presents the model Hamiltonian formulation within a two-level approximation, clarifies the control parameters, and analyzes topological qubit-state dynamics under biharmonic driving and strong curved confinement using the rotating-wave approximation (RWA). This section emphasizes the energy spectrum, which exhibits two time-reversal-symmetric paths as revealed by the quasi-energy approach. This spectrum informs the analysis of Landau-Zener-Stückelberg (LZS) interferometry transitions under the specified driving protocol, which can generate a synthetic gauge field and enable novel Floquet topological phenomena [52]. Section III introduces a formalism for evaluating resonance transition probabilities between quantum states at avoided level crossings induced by topological qubit-state coupling. The topological geometric phase is derived for open systems in the

non-Abelian case. The analysis of chiral LZS interference patterns in this section omits dissipation. The study further investigates how fluctuations in resonance transition probabilities and time-reversal symmetry, as determined by the driving protocol, can be utilized to manipulate topological qubit states and calibrate pulses in the confinement-dominated regime. Section IV discusses additional implications of quantum technologies across various physical settings. Section V summarizes the results and provides concluding remarks.

## II. MODEL AND FLOQUET THEORY

A spin qubit in a three-dimensional hetero-structure magnetic quantum wire is considered. The system is subjected to a parabolic confinement potential of specified strength and a biharmonic electromagnetic field. It is described by the time-dependent Hamiltonian [53]:

$$\mathcal{H}_{LZSM}(t) = \frac{-h(t)}{2}\hat{\sigma}_z - \frac{\Delta}{2}\hat{\sigma}_x \quad (1)$$

where  $\hat{\sigma}_{x,z}$  are Pauli matrices,  $\Delta$  is the tunnelling matrix element, and the time-dependent bias is

$$h(t) = \gamma_1 + \gamma_2 \sin(\omega t) - \gamma_3 \cos(2\omega t + \theta), \quad (2)$$

The coefficients  $\gamma_i$  explicitly depend on the confinement  $\Omega$  and the magnetic field amplitudes ( $\alpha = \mu_B B_0$ ,  $\beta = \mu_B B$ ):

$$\gamma_1 = 1 + \frac{\alpha^2}{2\Omega^2} + \frac{\beta^2}{4\Omega^2}, \quad \gamma_2 = \frac{\alpha\beta}{\Omega} \quad \text{and} \quad \gamma_3 = \frac{\beta^2}{2\Omega}. \quad (3)$$

The direct coupling between spatial confinement and temporal drive parameters facilitates the novel effects described in this study. To analyse this periodically driven system, the Floquet formalism is employed [17, 18]. A canonical transformation is then applied:

$$|\psi(t)\rangle = \mathcal{V}_0(t)|\bar{\psi}(t)\rangle, \quad (4)$$

with

$$\mathcal{V}_0(t) = \exp\left[\frac{-i}{2\hbar}\phi(t)\sigma_z\right] \quad (5)$$

and

$$\phi(t) = \gamma_1 t + \frac{\gamma_2}{\hbar\omega} \cos(\omega t) - \frac{\gamma_3}{2\hbar\omega} \sin(2\omega t + \theta) + \sin\theta, \quad (6)$$

we derive a modified Hamiltonian. Using the Jacobi-Anger expansion and applying the rotating-wave approximation (RWA) near resonances:

$$\frac{\gamma_1}{\hbar} + (n + 2m)\omega \approx 0 \quad (7)$$

we obtain the effective Rabi frequency:

$$\Delta_r(\Omega, \theta) = \exp\left(-i\frac{\gamma_3}{2\hbar\omega} \sin\omega\right) \frac{\Delta}{2} \sum_{n=-\infty}^{\infty} \sum_{m=-\infty}^{\infty} j_n\left(\frac{\gamma_2}{\hbar\omega}\right) j_m\left(\frac{\gamma_3}{\hbar\omega}\right) \exp(-im\theta). \quad (8)$$

The quasi-energies in this RWA are:

$$\mathcal{E}_{1,2} = \pm|\Delta_r(\Omega, \theta)|/2. \quad (9)$$

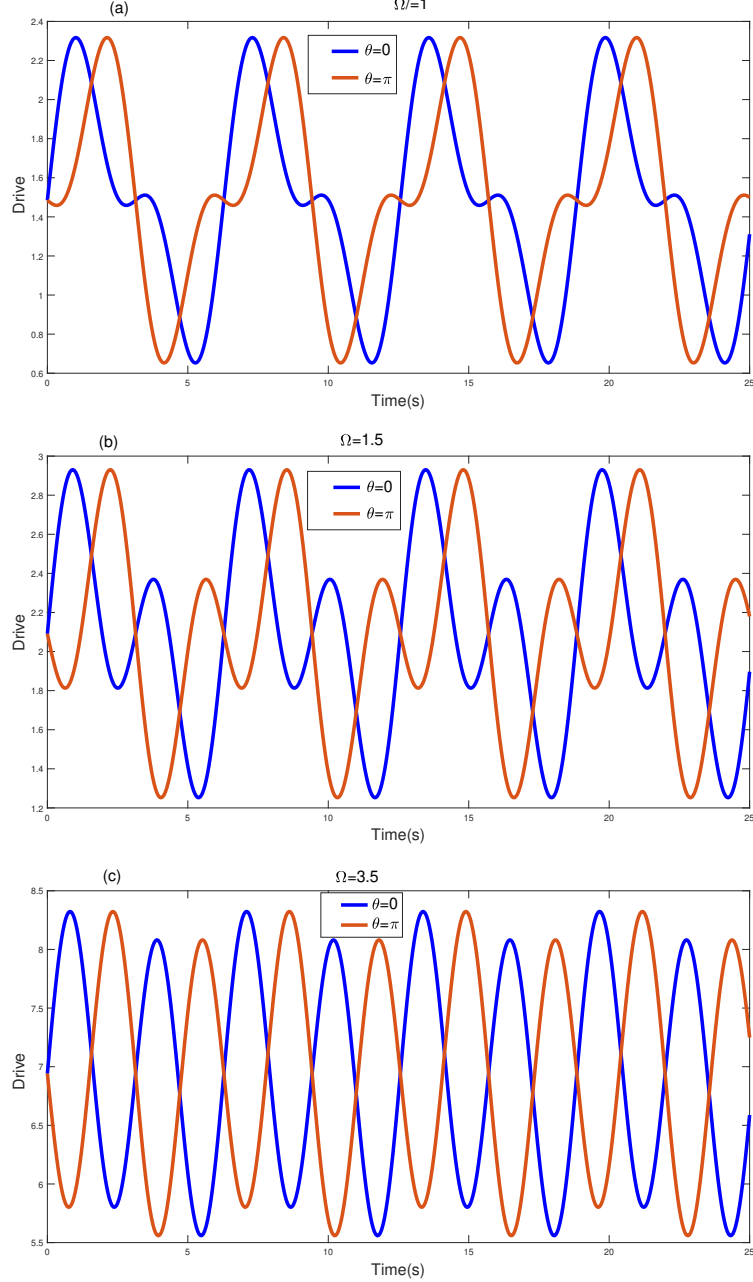


Figure 1. (Color online) Drive waveform for different values of a curved confinement (a)  $\Omega = 1$ , (b)  $\Omega = 1.5$ , and (c)  $\Omega = 3.5$  when the drive asymmetry parameter is fitted at  $\theta = 0$  and  $\theta = \pi$ . We have observed that the waveform becomes asymmetric in time when  $\theta \neq 0$ . However, as the curved confinement increases, consecutive phases of the drive signal will lead to a buildup of excited-state population. The system parameters used here are  $\omega = 1$  rad/s,  $\alpha = 0.5$  and  $\beta = 1.2$

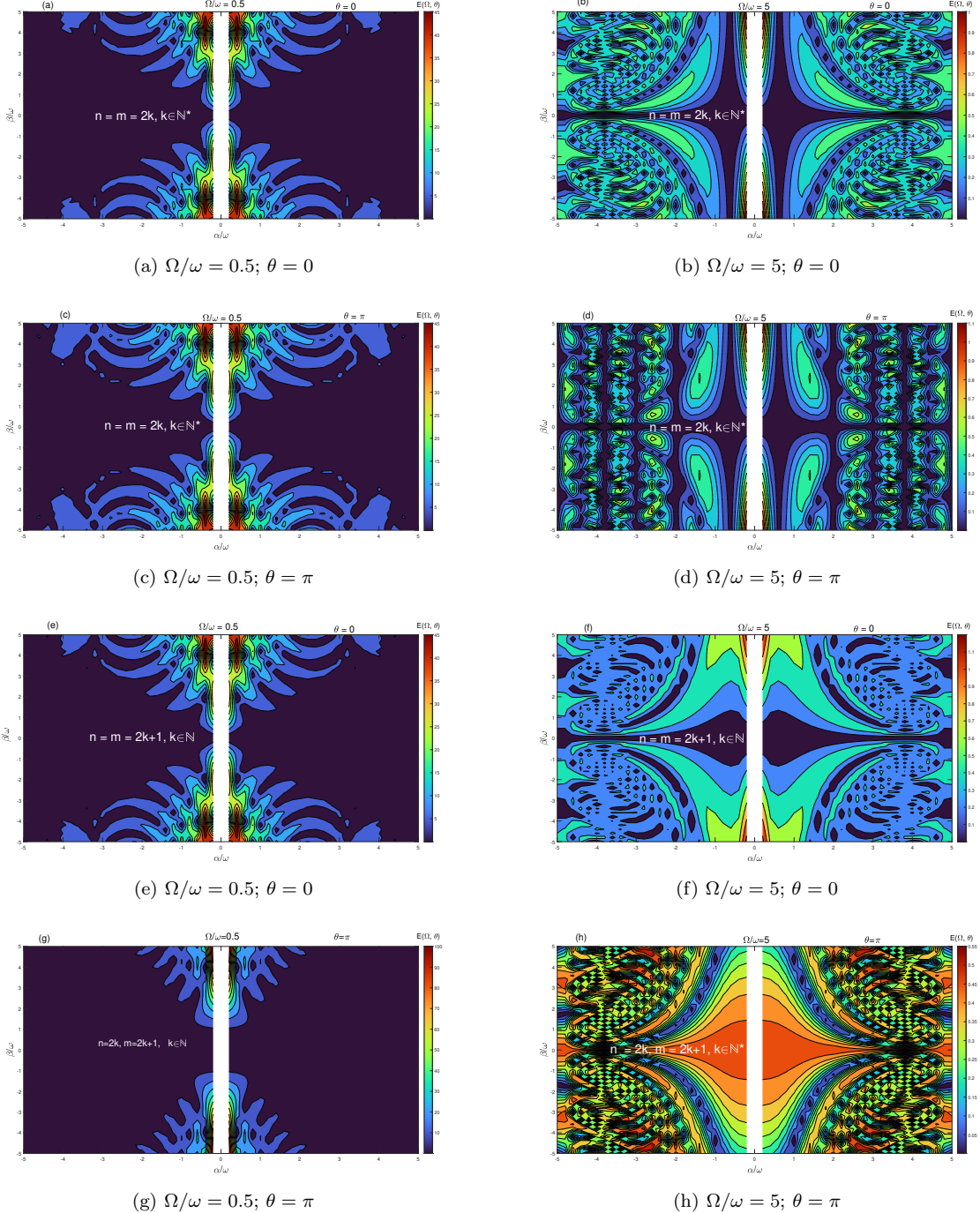


Figure 2. (Color online) Quasi-energy levels waveform for different values of the a curved confinement  $\Omega/\omega = 0.5$ , (b)  $\Omega/\omega = 5$  when the drive asymmetry parameter is fitted respectively at (a), (b)  $\theta = 0$  and (c), (d)  $\theta = \pi$  (by a set of  $n = m = 2k$ , with  $k \in \mathbb{N}^*$ ). Other parameters utilized in this study are  $\omega = 1\text{rad/s}$  and  $\Delta = 0.47$ .

### A. Synthetic Gauge Field and Non-Abelian Structure

The factor  $\exp(-i\Theta)$  in Eq (8), where  $\Theta = \frac{\gamma_3}{2\hbar\omega} \sin \omega t + m\theta$ , represents a synthetic gauge potential  $\mathcal{A}(\theta) = \hbar \nabla_\theta \Theta$ . The corresponding synthetic magnetic field is:

$$\mathcal{B} = \nabla_\theta \times \mathcal{A} \propto \frac{\gamma_3}{\hbar\omega} \cos \omega t + const. \quad (10)$$

For multi-level systems or qubit arrays, this gauge structure becomes non-Abelian, enabling the generation of non-Abelian geometric phases [41, 54] under adiabatic evolution in the  $(\Omega, \theta)$  parameter space.

The geometric character, defined in terms of geometrical qubits, of the non-Abelian topological geometric phase is evident from the phase factor, which depends solely on the path rather than its parametrization. Notably, the nontrivial geometric phases arising after topological transitions are considered in the analysis of constructive and destructive interference of wave functions under the Floquet mechanism. In this context, the underlying symmetry of the degenerate subspace  $(\Omega, \theta)$ , results in a non-Abelian gauge field structure. Gauge fields generated by optical fields originate from the redistribution of photons among different plane wave modes. Furthermore, the influence of the gauge field imprinted on the qubit is examined in relation to its internal state dynamics.

## III. RESULTS AND DISCUSSION

### A. Topological Transition and Chiral Interference

Figure 1 presents the driving waveform  $h(t)$  for various confinement strengths. At low confinement ( $\Omega/\omega = 1$ ), the waveform displays pronounced asymmetry for  $\theta \neq 0$ . As  $\Omega/\omega$  increases ( $\Omega/\omega = 3.5$ ), waveform symmetry is restored, indicating confinement-mediated symmetry control. In panel (c), Bloch oscillations are tracked diabatically, and the system occupies a superposition of states in both the lower and upper bands. Deviations from asymmetric to symmetric wave packets may arise due to LZ transitions at unavoidable wave touchings. These transitions result from quantum superposition near avoided crossings, with the LZ transition probability governed by the interwave coupling strength [53]. The period of the topological drive protocol is comparable to the qubit's dephasing timescale, and coherence is maintained within the modulation topological phase as the curved confinement increases. Numerical investigations of non-adiabatic transitions at these wave-touchings and their influence on unconventional Bloch oscillations suggest potential for tunable quantum-transport applications. These methods are further applied to examine the relationship between irregular Bloch oscillations and tunneling parameters in a parabolic quantum wire under biharmonic driving. This conclusion is supported by the agreement between experimental results, analytical theory, and simulations.

Figure 2 displays the quasi-energy spectrum  $(\alpha/\omega, \beta/\omega)$ . Under low confinement conditions (Figs. 2a, 2c), the spectrum exhibits symmetric interference fringes as the system transitions through even parameters ( $n = m = 2k$ , where  $k$  is a positive integer). In contrast, high confinement (Figs. 2b, 2d) results in a significant reconstruction, with chiral, vortex-like structures emerging for odd parameters ( $n = m = 2k+1$ ). This confinement-induced topological transition is marked by a change in the Chern number of the Floquet bands, analogous to Floquet Chern insulators [55, 56]. The interplay between geometric deformation at  $(n = m = 2k+1)$  and the symmetries of these interference fringes fundamentally influences the electronic band structure of the qubit states. These results have important implications for understanding and potentially controlling optical responses in tunable photonic devices, offering insight into the influence of

irregular Bloch oscillation patterns on the manipulation of the quantum confinement parameter ( $\Omega/\omega$ ). Geometric frustration at ( $\alpha/\omega = 0, \beta/\omega = 0$ ) leads to destructive interference, resulting in localized qubit states. These observations can often be extended to higher-dimensional systems along high-symmetry paths within the Brillouin zone, providing a broader perspective on electronic transport in complex structures.

### B. Non-Abelian Geometric Phases and Holonomic Quantum Computation

This study presents a novel approach to the Floquet problem for a dynamically driven two-level system (TLS) under the influence of a biharmonic electromagnetic field. The analysis demonstrates that each periodic solution of the transition probability, including those that are time-reversal symmetric in subspaces ( $\alpha/\omega, \beta/\omega$ ), produces well-defined intermediate states of the driven system with tunable amplitude. This framework facilitates the identification of resonance transition characteristics arising from the motion and crossing of quasi-energy levels. The existence of a Floquet solution to the original Schrödinger equation,

$$\hbar|\psi(t)\rangle = \mathcal{H}(t)|\psi(t)\rangle, \quad (11)$$

which can be explicitly determined through integration, is presented as follows:

$$\hbar|\psi(t)\rangle = v(t, t_0)|\psi(t_0)\rangle, \text{ where, } v(t, t_0) = \hat{P} \exp\left(-\frac{i}{\hbar} \int_{t_0}^t \mathcal{H}(\tau) d\tau\right). \quad (12)$$

The symbol  $\hat{P}$  represents the time-ordering operator. Floquet time evaluation in periodically driven quantum systems entails analyzing the system's behavior over a complete cycle ( $T$ ) using the Floquet time-evolution operator  $v(t, t_0)$ , which maps the quantum state from the beginning to the end of the period. The eigenvalues of the Floquet operator can be represented as follows:

$$v(T)|\Phi_k(t)\rangle = \exp\left(-i\frac{E_k}{\hbar}\right), \text{ and } |\Phi_k(t+T)\rangle = |\Phi_k(t)\rangle, \quad (13)$$

$v(T)$  facilitates the identification of time-independent Floquet states (quasienergy states) and their associated quasienergies. Such an approach simplifies the analysis, particularly in regimes of slow or fast driving, as well as in applications such as quantum pumping and Floquet engineering. Additionally, point-map analysis of system states after each period can reveal whether dynamics are stable or chaotic.

Adiabatic cyclic evolution in the  $(\Omega/\omega, \theta)$  parameter space generates non-Abelian geometric phases. In a three-level system, such as a triple quantum dot or a three-qubit array, the synthetic gauge potential  $\mathcal{A}$  becomes matrix-valued. The resulting holonomy, defined by the path-ordered exponential  $\hat{P} \exp\left(-\frac{i}{\hbar} \int_{t_0}^t \mathcal{H}(\tau) d\tau\right)$ , enables non-Abelian geometric quantum computation [19, 23]. Path-dependent holonomic gates have been implemented using this method [34, 41, 57, 58]. Quantum information is encoded in a set of degenerate eigenstates of the parameter-dependent Hamiltonian, and the qubit states are then adiabatically driven to evolve cyclically in the  $(\Omega/\omega, \theta)$  parameter space. This method provides inherent robustness against biharmonic electromagnetic field noise, as demonstrated in recent superconducting qubit experiments [24].

### C. Floquet-Bloch Oscillations in Phase Space

Figure 2 presents the quasi-energy  $E$  as a function of the phase  $\theta$  for a fixed driving amplitude. At high confinement ( $\Omega/\omega = 5$ , Fig. 3b), the quasi-energy levels display pronounced oscillatory

behavior, known as Floquet-Bloch oscillations, with  $\theta$  serving as a synthetic crystal momentum. These oscillations directly indicate the engineered gauge structure and constitute a novel form of coherent transport in parameter space, which may have applications in quantum sensing [25]. Notably, a transition from even parameters ( $n = m = 2k$ , where  $k$  is a positive integer, as shown in Fig. 2(a), 2(b), 2(c), and 2(d)) to odd parameters ( $n = m = 2k + 1$ , where  $k$  is an integer, as shown in Fig. 2(e), 2(f), 2(g), and 2(i)) reveals new symmetric patterns in the dependence of quasi-energy on the relative quantum confinement parameter  $\Omega/\omega$  and the phase  $\theta$ . Each mode serves as an initial condition for a set of sideband coherent transport phenomena.

Colored waveguides illustrate the site heterostructure magnetic quantum wire, which exhibits two quasi-energies of equal magnitude but opposite phase in uniform Floquet-Bloch oscillations. Adjusting system parameters, such as  $\Omega/\omega$  or  $\theta$ , can induce either destructive or constructive interference in neighboring  $\mathcal{A}(\Theta)$  sites. The band degeneracy is lifted, resulting in the emergence of gaps between the colored flatband and dispersive bands at  $\alpha/\omega$ . Determining the population probabilities of the system levels requires analysis of the quasi-energy spectrum. Previous studies [13, 15, 18, 19, 40, 42] have demonstrated that this method accurately characterizes intermediate states of the driven system at optimal amplitude and facilitates the identification of resonance transitions arising from the dynamics and crossing of quasi-energy levels. When such crossings occur, the transition probability may increase significantly due to the acquisition of a time-independent component. In general, quasi-energy crossings exert a substantial influence on the population distribution among levels in complex quantum systems[29, 30].

The numerical results presented in Fig. 2 exhibit strong agreement, which is particularly noteworthy considering the numerical instabilities that arise when solving Eq. (8) as a result of the highly oscillatory behavior of the Bessel function. These constraints introduce significant complexity to the analytical investigation of the resulting phases and amplitudes, a topic that lies beyond the scope of this study. Under resonance conditions, exact cancellations of destructive interference are observed along the driving parameter plane ( $\alpha/\omega = 0, \beta/\omega = 0$ ) when  $j_n(\frac{\gamma_2}{\hbar\omega}) = 0$  or  $j_m(\frac{\gamma_3}{\hbar\omega}) = 0$ . This observation is essential for elucidating the emergence of LZS interferometry transitions under the applied driving protocol.

#### D. Robust Multiphoton Transitions and Dynamical Decoupling

The parameters  $E_k$  are referred to as quasi-energies in the present system, where  $k = 1, 2$ . These eigenvalues  $E_k$  can be mapped into the first Brillouin zone, such that  $-\hbar\omega/2 < E_k < \hbar\omega/2$ . In the quasi-energy basis  $|\Phi_k(t)\rangle$ , the transition probability  $P_{|\downarrow\rangle \rightarrow |\uparrow\rangle}(t, t_0)$  is given by

$$P_{|\downarrow\rangle \rightarrow |\uparrow\rangle}(t, t_0) = \sum_{k,l} \exp(-i(E_k - E_l)(t - t_0)/\hbar) A_k(t, t_0) A_l^*(t, t_0), \quad (14)$$

where,  $A_k(t, t_0) = \langle \uparrow | \Phi_k(t) \rangle \langle \Phi_k | \downarrow \rangle$ . Eq. (14) provides the probability of a transition from the initial qubit state  $|\downarrow\rangle$  to the final quantum state  $|\uparrow\rangle$ , incorporating quantum superposition summed over  $l$ . The result is subsequently summed over all final field states (summed over  $k$ ). At this stage, contributions with different  $k$  and  $l$  values exhibit pronounced oscillations, thereby diminishing the overall transition probability. Modifying system parameters, such as the curved confinement  $\Omega$  of the wire can bring two quasi-energies close to degeneracy,  $E_k = E_l$ . Under these circumstances, the transition probability increases substantially. Therefore, the principal quantity of interest is the transition probability averaged over initial times  $t_0$ , while keeping the elapsed time  $t - t_0$  fixed. This average can be directly obtained from Eq. (14), providing the

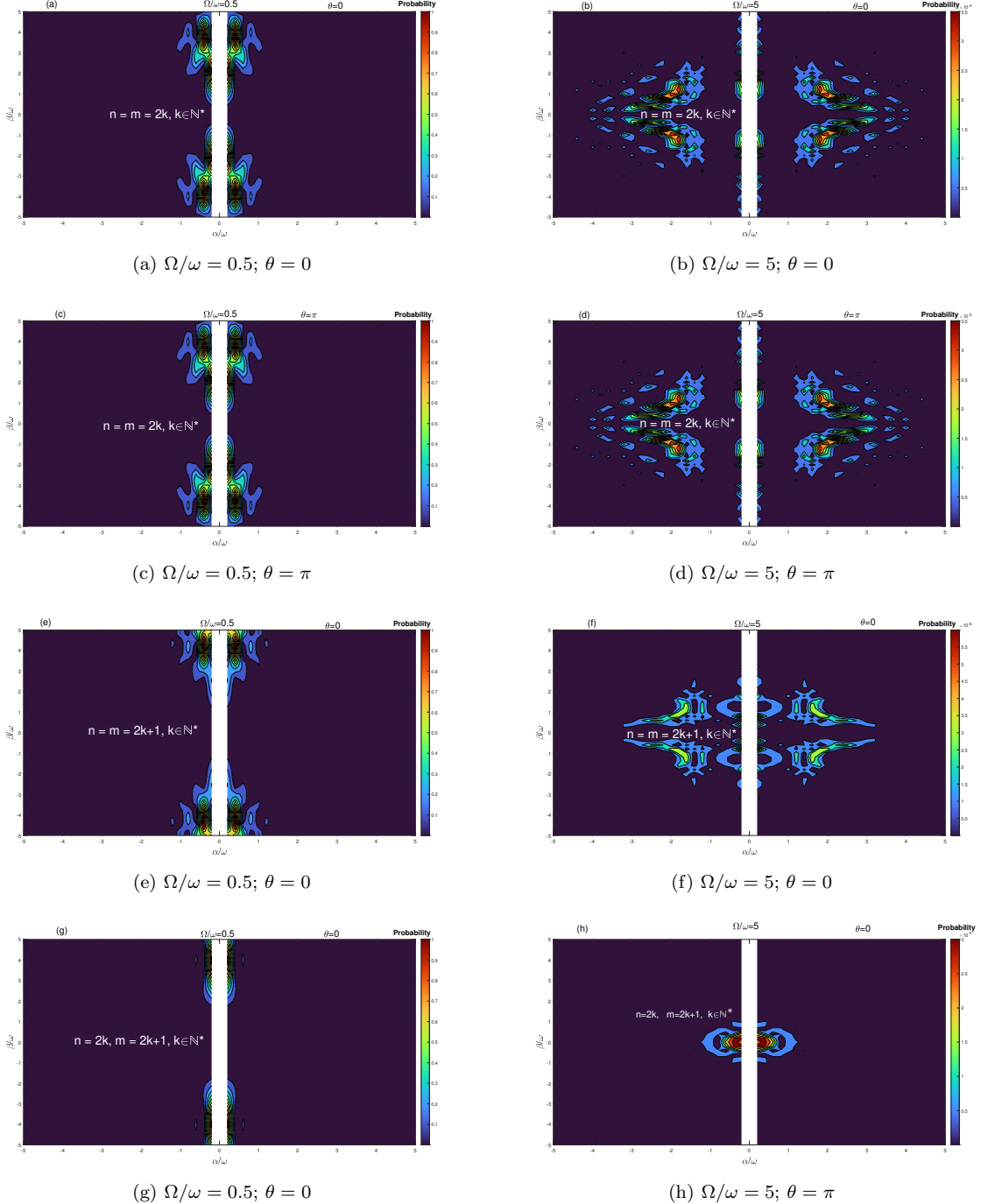


Figure 3. (Color online) The probability  $P_{|\downarrow\rangle\rightarrow|\uparrow\rangle}$  is shown as functions of  $\theta$ , the driving amplitude ( $\alpha/\omega, \beta/\omega$ ) plan for  $\Omega/\omega = 0.5$  in (a, c, e and g) and  $\Omega/\omega = 5$  in (b, d, f and h). The system parameters utilized in this study are  $\Delta = 0.47$  and  $\alpha/\omega = 4.4$ .

required result

$$P_{|\downarrow\rangle \rightarrow |\uparrow\rangle}(t, t_0) = \sum_k \sum_{n,l} \left| \langle \uparrow | \Phi_k^{(n-l)} \rangle \right|^2 \left| \langle \Phi_k^{(n-l)} | \downarrow \rangle \right|^2 \quad (15)$$

where calculations  $\Phi_k^{(n)} = \frac{1}{T} \int_0^T \exp(i\omega t) \Phi_k(t) dt$  are the Fourier components of the quasi-energy function. Eq. (15) is simply a generalization of the Rabi formula long used by workers in atomic and molecular beam resonance spectroscopy [59]. Considering only the resonant term in the  $k$  and  $n$  sum of Eq. (15) in Ref. [46], the probability to go from a single initial Floquet state  $|\downarrow, 0\rangle$  to a final Floquet  $|\uparrow, k\rangle$ , summed over all  $k$  in the RWA, is given by

$$P_{|\downarrow, 0\rangle \rightarrow |\uparrow, k\rangle}(t, t_0) = \frac{1}{2} \frac{|\Delta_r^2|}{\mathcal{E}_{nm}^2} \left[ 1 - \cos(\mathcal{E}_{nm}(t))t \right]. \quad (16)$$

When we look at how the Bessel functions behave for large values in formula (8) for the Rabi frequency, the product of the Bessel functions, as shown in [24], becomes:

$$j_n\left(\frac{\gamma_2}{\hbar\omega}\right)j_m\left(\frac{\gamma_3}{\hbar\omega}\right) = \frac{2\hbar\omega}{\pi\gamma_2} \sqrt{\frac{2}{\gamma_3}} \left\{ \cos\left[\frac{\gamma_2}{\hbar\omega}\left(1 - \frac{\gamma_3}{2}\right) - \frac{\pi}{2}(n-m)\right] \right. \\ \left. + \sin\left[\frac{\gamma_2}{\hbar\omega}\left(1 + \frac{\gamma_3}{2}\right) - \frac{\pi}{2}(n+m)\right] \right\}. \quad (17)$$

The transition probability  $P_{|\downarrow\rangle \rightarrow |\uparrow\rangle}$  (Fig. 3) illustrates confinement-induced resonance filtering at high  $\Omega/\omega$  (Figs. 3a, 3c, 3e, 3g), where specific multiphoton channels are selectively enhanced, with probabilities approaching unity due to band structure symmetry. The frequency of LZS interference is derived as a function of the driving parameters using Floquet theory. Constructive interference from time-reversed paths leads to reduced curved confinement, provided the parity mode conditions for  $n$  and  $m$  are satisfied. The analysis follows the instantaneous eigenstate that begins in  $|\downarrow\rangle$  and ends in  $|\uparrow\rangle$ , thereby minimizing excitation of  $|\uparrow\rangle$ . Mixing two drives with distinct topological phases produces phase-dependent qubit populations. The control and measurement protocol involves observing coherent multiphoton resonances between discrete states to classify topological phases. Few-qubit state transitions occur at high photon orders according to the parity mode  $n = m = 2k$  and  $n = m = 2k + 1$ , at  $k \in \mathbb{N}^*$ . Specifically, the qubit state transition shifts to  $\theta = \pi$  with lower probability, leading to a plateau in the symmetric transition probabilities. Sudden configuration changes are observed from an almost unaltered state (3b; 3d; 3f) to interband transitions while conserving the symmetric cell. As curved confinement increases, the beam intensity exhibits an asymmetric energy distribution. This behavior provides inherent robustness against fluctuations in drive amplitude, addressing a significant challenge in quantum control [60].

The confinement-induced topological phase in the environment offers significant advantages for achieving high-fidelity and robust quantum gates. The observed population trapping, which depends on the relative phase difference  $\theta$  between the drives (blue trajectories in Figs. 4b, 4d), facilitates high-fidelity state transfer and dynamic decoupling from specific noise channels. As indicated by Eq. (4), a biharmonic drive exhibits sensitivity to the topological phase, as shown in Figs. 4b and 4d. Figure 4 demonstrates that the maxima and minima are symmetrically distributed. Increasing the confinement frequency can stabilize the population of a qubit in its excited state, and minor variations in the curved confinement do not significantly affect this stability. Additionally, LZ Bloch band oscillations display notable characteristics, including an asymmetric quasienergy distribution at specific biharmonic field parameters. As a result, the number of scatterers increases, and the properties of the incoming and outgoing leads are

strongly influenced by the geometry of the quantum wire, which in turn affects the transition probabilities in LZSM interferometry.

The theory is further extended to investigate the relationships among irregular Floquet Bloch oscillations, band structure, and tunneling phenomena in novel quantum-wire materials. While these materials exhibit topological equivalence under certain symmetry transformations, they differ in spatial band connectivity and dispersion, particularly under curved confinement strain. Due to the complex space-band structure, the wave packet is amplified each time it traverses asymmetric cells at high values of  $\Omega/\omega$ . Although the asymmetry of the interference pattern is not emphasized here, adjusting the curved confinement parameters enables control over the LZSM interferometry transition, which is significant for managing qubit state dynamics. Moreover, the structural band symmetries of specific multiphoton channels are intrinsically connected to their topological properties, indicating potential applications in optoelectronic and quantum transport devices [61].

The emergence and characteristics of irregular configuration space bands in quantum wire materials, which exhibit distinct Floquet Bloch oscillation topologies, require further investigation. These results may be generalized to higher-dimensional systems along high-symmetry paths within the Brillouin zone, thereby providing a broader understanding of electronic transport in complex lattice structures [62–64].

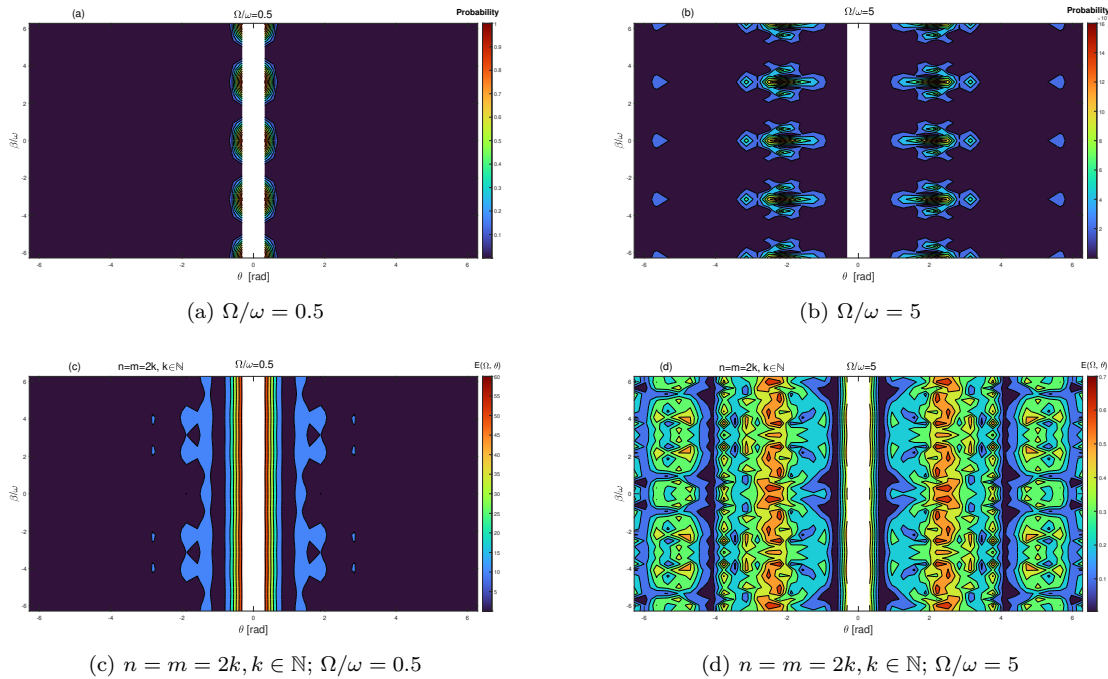


Figure 4. (Color online) The probability  $P_{|\downarrow\rangle\rightarrow|\uparrow\rangle}$  of the excited state  $|\uparrow\rangle$  and the quasi-energy versus the different phase  $\theta$  and the driving amplitude  $\beta/\omega$  plan:  $\Omega/\omega = 0.5$  (a, c) and  $\Omega/\omega = 5$  in (b, d). The system parameters utilized here are:  $\Delta = 0.47$  and  $\alpha/\omega = 4.4$

#### IV. IMPLICATIONS FOR QUANTUM TECHNOLOGIES

The validity of a theoretical model is determined by its comparison to experimental data, where it is established and evaluated based on the significance of the results obtained. This paper examines the Floquet Hamiltonian and the effective Hamiltonians generated by periodic driving. Floquet theory significantly influences the system's dynamics during numerical computations. The present findings have profound implications for quantum technologies:

- **Holonomic Quantum Computation:** The observed non-Abelian geometric phases in quantum wire materials enable holonomic quantum computation [41], offering inherent resilience to control errors.
- **Floquet Topological Matter:** Arrays of quantum wire materials subjected to biharmonic driving can simulate exotic topological phases [65], such as Floquet-Weyl semimetals [66].
- **Quantum Metrology:** The pronounced sensitivity of interference patterns to external parameters renders this system suitable for advanced quantum sensing applications [67, 68].
- **Fault-Tolerant Quantum Gates:** The integration of geometric phases with dynamical decoupling facilitates the design of fault-tolerant quantum gates as discussed in [69] and other references therein.

#### V. CONCLUSION

Theoretical analysis shows that the interplay between tunable curved confinement and biharmonic driving in quantum-wire materials generates a diverse range of Floquet topological phenomena. Key findings include a confinement-induced topological transition, the emergence of non-Abelian geometric phases, and Floquet Bloch oscillations in parameter space. These results position quantum-wire materials as a versatile platform for topological quantum control and fault-tolerant quantum information processing. The experimental realization of these effects is feasible with current nano-fabrication and microwave control technologies.

#### ACKNOWLEDGMENTS

This work was supported by the Organization for Women in Science for the Developing World (OWSD) and the Swedish International Development Cooperation Agency (SIDA).

---

[1] D. Loss and D. P. DiVincenzo, [Quantum computation with quantum dots](#), *Phys. Rev. A* **57** (1998) 120.

[2] R. Hanson, L. P. Kouwenhoven, J. R. Petta, S. Tarucha, and L. M. K. Vandersypen [Spins in few-electron quantum dots](#), *Rev. Mod. Phys.* **79** (2007) 1217.

[3] C. Kloeffel and D. Loss, [Prospects for Spin-Based Quantum Computing in Quantum Dots](#), *Annu. Rev. Condens. Matter Phys.* **4** (2013) 51.

[4] O. Auslaender, A. Yacoby, R. de Picciotto, K.W. Baldwin, L. N. Pfeiffer, K. W. West, [Tunneling spectroscopy of the elementary excitations in a one-dimensional wire](#), *Science* **295** (2002) 825-828.

[5] Y. Tserkovnyak, B.I. Halperin, O. M. Auslaender, A. Yacoby, [Finite-size effects in tunneling between parallel quantum wires](#), *Phys. Rev. Lett.* **89** (2002) 136805.

[6] Y. Tserkovnyak, B. I. Halperin, O. M. Auslaender, A. Yacoby, [Interference and zero bias anomaly in tunneling between Luttinger-liquid wires](#), *Phys. Rev. B* **68** (2003) 125312.

- [7] O. M. Auslaender, H. Steinberg, A. Yacoby, Y. Tserkovnyak, B. I. Halperin, K.W. Baldwin, L. N. Pfeiffer, K.W. West, [Spin-charge separation and localization in one dimension](#), *Science* **308** (2005) 88-92.
- [8] H. Steinberg, G. Barak, A. Yacoby, L. N. Pfeiffer, K.W. West, B. I. Halperin, K. Le Hur, [Charge fractionalization in quantum wires](#), *Nat. Phys.* **4** (2008) 116-119.
- [9] M. Okuda, [Electrostatically controlled double-quantum-wire electron interferometers](#), *Appl. Phys.* **78** (1998) 1039
- [10] D. O. Shendryk, O. V. Ivakhnenko ,S. N. Shevchenko and Franco Nori, [Efficient implementation of quantum signal processing via the adiabatic-impulse model](#), *Phys. Rev. A.* **112** (2025) 042437.
- [11] T. Oka and S. Kitamura, [Floquet Engineering of Quantum Materials](#), *Annu. Rev. Condens. Matter Phys.* **10** (2019) 387.
- [12] M. S. Rudner and N. H. Lindner, [Band structure engineering and non-equilibrium dynamics in Floquet topological insulators](#), *Nat. Rev. Phys.* **2** (2020) 229.
- [13] M. Bukov, L. D'Alessio, and A. Polkovnikov, [Universal high-frequency behavior of periodically driven systems: from dynamical stabilization to Floquet engineering](#), *Adv. Phys.* **64** (2015) 139.
- [14] S. Shevchenko, S. Ashhab, and F. Nori, [Landau-Zener-Stückelberg interferometry](#), *Physics Reports* **492** (2010) 1.
- [15] F. Forster, G. Petersen, S. Manus, P. Hänggi, D. Schuh, W. Wegscheider, S. Kohler, and S. Ludwig, [Characterization of Qubit Dephasing by Landau-Zener-Stückelberg-Majorana Interferometry](#), *Phys. Rev. Lett.* **112** (2014) 116803.
- [16] A. Pedersen, L. Pizzagalli, and H. Jónsson, [Optimal atomic structure of amorphous silicon obtained from density functional theory calculations](#), *New J. Phys.* **19** (2017) 063018.
- [17] J. E. Danga, S. C. Kenfack, L. C. Fai, [Quantum wire and magnetic control of a spin qubit in the Landau-Zener-Stückelberg interferometry transition](#), *J. Phys. A Math. Theor.* **49** (2016) 195306.
- [18] J. E. Danga, C. Kenfack Sadem, M. N. Jipdi, A. J. Fotue, L. C. Fai, [Landau-Zener tunneling and magnetic control of spin qubit in a quantum wire: dynamic matrix approach](#), *Physica B* **515** (2017) 75-81
- [19] S. E. Mkam Tchouobiap, J. E. Danga, R. M. Keumo Tsiaze, L. C. Fai, [Coherent nonlinear low-frequency Landau-Zener tunneling induced by magnetic control of a spin qubit in a quantum wire](#), *Int. J. Qual. Innovat.* **6** (2018) 1850049
- [20] J.E. Danga, C. Kenfack Sadem, R.M. Keumo Tsiaze, L.C. Fai, [Landau-Zener tunneling of qubit states and Aharonov-Bohm interferometry in double quantum wires](#), *Physica E* **108** (2019) 123-134.
- [21] W. D. Oliver, Y. Yu, J. C. Lee, K. K. Berggren, L. S. Levitov, and T. P. Orlando, [Mach-Zehnder Interferometry in a Strongly Driven Superconducting Qubit](#), *Science* **310** (2005) 1653.
- [22] D. M. Berns, W. D. Oliver, S. O. Valenzuela, A. V. Shytov, K. K. Berggren, L. S. Levitov, and T. P. Orlando, [Coherent Quasiclassical Dynamics of a Persistent Current Qubit](#), *Phys. Rev. Lett.* **97** (2006) 150502.
- [23] A. M. Satanin, M. V. Denisenko, A. I. Gelman, and F. Nori, [Amplitude and phase effects in Josephson qubits driven by a biharmonic electromagnetic field](#), *Phys. Rev. B* **90** (2014) 104516.
- [24] R. Blattmann, P. Hanggi, and S. Kohler, [Qubit interference at avoided crossings: The role of driving shape and bath coupling](#), *Phys. Rev. A* **91** (2015) 042109.
- [25] J. Q. You and F. Nori, [Superconducting Circuits and Quantum Information](#), *Phys. Today* **58**(11) (2005) 42.
- [26] J. Q. You and F. Nori, [Atomic physics and quantum optics using superconducting circuits](#), *Nature* **474** (2011) 589.
- [27] M. Sillanpaa, T. Lehtinen, A. Paila, Yu. Makhlin, and P. Hakonen, [Continuous-Time Monitoring of Landau-Zener Interference in a Cooper-Pair Box](#), *Phys. Rev. Lett.* **96** (2006) 187002.
- [28] C. M. Wilson, T. Duty, F. Persson, M. Sandberg, G. Johansson, and P. Delsing, [Coherence Times of Dressed States of a Superconducting Qubit under Extreme Driving](#), *Phys. Rev. Lett.* **98** (2007) 257003.
- [29] A. Izmalkov, S. H. W. van der Ploeg, S. N. Shevchenko, M. Grajcar, E. Il'ichev, U. Hubner, A. N. Omelyanchouk, and H.-G. Meyer, [Consistency of Ground State and Spectroscopic Measurements on Flux Qubits](#), *Phys. Rev. Lett.* **101** (2008) 017003.
- [30] S. Gasparinetti, P. Solinas, and J. P. Pekola, [Geometric Landau-Zener Interferometry](#), *Phys. Rev. Lett.* **107** (2011) 207002.

- [31] D. M. Berns, M. S. Rudner, S. O. Valenzuela, K. K. Berggren, W. D. Oliver, L. S. Levitov, T. P. Orlando, **Amplitude spectroscopy of a solid-state artificial atom**, *Nature* **455** (2008) 51.
- [32] M. S. Rudner, A. V. Shytov, L. S. Levitov, D. M. Berns, W. D. Oliver, S. O. Valenzuela, and T. P. Orlando, **Quantum Phase Tomography of a Strongly Driven Qubit**, *Phys. Rev. Lett.* **101** (2008) 190502.
- [33] N. H. Lindner, G. Refael and V. Galitski, **Floquet topological insulator in semiconductor quantum wells**, *Nat. Phys.* **7** (2011) 490-495.
- [34] F. Wilczek and A. Zee, **Appearance of gauge structure in simple dynamical systems**, *Phys Rev Lett* **52** (1984) 2111.
- [35] R. Moessner and S. Sondhi, **Equilibration and order in quantum Floquet matter**, *Nat. Phys.* **13** (2017) 424.
- [36] C. Weitenberg and J. Simonet, **Tailoring quantum gases by Floquet engineering**, *Nat. Phys.* **17** (2021) 1342.
- [37] H. Zhou, J. Choi, S. Choi, R. Landig, A. M. Douglas, J. Isoya, F. Jelezko, S. Onoda, H. Sumiya, P. Cappellaro, H. S. Knowles, H. Park, and M. D. Lukin, **Quantum metrology with strongly interacting spin systems**, *Phys. Rev. X* **10** (2020) 031003.
- [38] L. J. Fiderer and D. Braun, **Quantum metrology with quantum chaotic sensors**, *Nat. Commun.* **9** (2018) 1351.
- [39] M. Jiang, H. Su, Z. Wu, X. Peng, and D. Budker, **Floquet maser**, *Sci. Adv.* **7**, (2021) 8.
- [40] J. Pachos and P. Zanardi, **Quantum Holonomies for Quantum Computing**, *International journal of modern Physics B* **15** (2001) 1257.
- [41] P. Zanardi and M. Rasetti, **Holonomic quantum computation**, *Phys. Lett. A* **264** (1999) 94-99.
- [42] J. Pachos, P. Zanardi, and M. Rasetti, **Non-Abelian Berry connections for quantum computation**, *Physica Review A* **61** (1999) 010305(R).
- [43] H. Wu, G. Heinrich and F. Marquardt, **The effect of Landau-Zener dynamics on phonon lasing**, *New J. Phys.* **15** (2013) 123022.
- [44] Xueda Wen and Yang Yu, **Landau-Zener interference in multilevel superconducting flux qubits driven by large-amplitude fields**, *Phys. Rev. B* **79** (2009) 094529.
- [45] M. O. Scully and M. S. Zubairy, **Quantum Optics**, (Cambridge University Press, Cambridge, 1997).
- [46] J. H. Shirley, **Solution of the Schrödinger Equation with a Hamiltonian Periodic in Time**, *Phys. Rev.* **138** (1965) B979.
- [47] J. A. Jones, V. Vedral, A. Ekert, and G. Castagnoli, **Geometric quantum computation using nuclear magnetic resonance**, *Nature* **403** (2000) 869-871.
- [48] Lu-Ming Duan, Juan I Cirac, and Peter Zoller, **Geometric manipulation of trapped ions for quantum computation**, *Science* **292** (2001) 1695-1697.
- [49] P. Solinas, M. Sasetti, P. Truini, and N. Zanghi, **On the stability of quantum holonomic gates**, *New. J. Phys.* **14** (2012) 093006.
- [50] C. Zener, in *Proceedings of the Royal Society of London A: Mathematical, Physical and Engineering Sciences*, Vol. **137** (The Royal Society, 1932) pp. 696-702.
- [51] R. Khomeriki and S. Flach, **Landau-Zener Bloch Oscillations with Perturbed Flat Bands**, *Phys. Rev. Lett.* **116** (2016) 245301.
- [52] A. A. Silaev and N. V. Vedenskii, **Residual-Current Excitation in Plasmas Produced by Few-Cycle Laser Pulses**, *Phys. Rev. Lett.* **102** (2009) 115005.
- [53] J. E. Danga, C. Kenfack-Sadem, M. N. Jipdi, A. J. Fotue and L. C. Fai, **Landau-Zener tunneling and magnetic control of spin qubit in a quantum wire: Dynamic matrix approach**, *Physica B: Condensed Matter* **515** (2017) 75-81.
- [54] Erik Sjöqvist, **Geometric phases in quantum information**, *Int. J. Quant. Chem.* **115** (2015) 19, 1311-1326
- [55] M. S. Rudner and N. H. Lindner, **Band structure engineering and non-equilibrium dynamics in Floquet topological insulators**, *Nat. Rev. Phys.* **2** (2020) 229-244.
- [56] T. Kitagawa, E. Berg, M. Rudner and E. Demler, **Topological characterization of periodically driven quantum systems**, *Phys. Rev. B* **82** (2010) 235114
- [57] Y. Aharonov, J. Anandan, **Phase change during a cyclic quantum evolution**, *Phys Rev Lett* **58** (1987) 1593-1596.
- [58] J. Anandan, **Non-adiabatic non-Abelian geometric phase**, *Phys Lett A* **133** (1988) 171-175.

- [59] P. Kusch and V. W. Hughes, in **Handbuch der Physik**, edited by S. Flugge (*Springer-Verlag, Berlin, 1959*), Vol. **37/1**, pp. 54-73
- [60] T. Chen, J-Q Hu, C. Zhang, and Z.-Y. Xue, **Universal robust geometric quantum control via geometric trajectory correction**, *Phys. Rev. Applied* **22** (2024) 014060.
- [61] Z. Liu, F. Liu and Y-S Wu, **Exotic electronic states in the world of flat bands: From theory to material**, *Chinese Phys. B* **23** (2014) 077308.
- [62] C. L. Kane and E. J. Mele, **Quantum Spin Hall Effect in Graphene**, *Phys. Rev. Lett.* **95** (2005) 226801.
- [63] M. Cristiani, O. Morsch, J. H. Müller, D. Ciampini, and E. Arimondo, **Experimental properties of Bose-Einstein condensates in one-dimensional optical lattices: Bloch oscillations, Landau-Zener tunneling, and mean-field effects**, *Phys. Rev. A* **65** (2002) 063612.
- [64] A. Yoichi, **Topological Insulator Materials**, *J. Phys. Soc. Jpn.* **82** (2013) 102001.
- [65] A. V. Yulin, I. A. Shelykh, E. S. Sedov, and A. V. Kavokin, **Spin resonance induced by a mechanical rotation of a polariton condensate**, *Phys. Rev. B* **108** (2023) 045301.
- [66] Z.-M. Wang, R. Wang, J.-H. Sun, T.-Y. Chen, and D.-H. Xu, **Floquet Weyl semimetal phases in light-irradiated higher-order topological Dirac semimetals**, *Phys. Rev. B* **107** (2023) L121407.
- [67] C. L. Degen, F. Reinhard, and P. Cappellaro, **Quantum sensing**, *Rev. Mod. Phys.* **89** (2017) 035002.
- [68] F. Dolde, H. Fedder, M. W. Doherty *et al.*, **Electric-field sensing using single diamond spins**, *Nat. Phys.* **7** (2011) 459-463.
- [69] A. Katabarwa, K. Gratsea, A. Caesura, and P. D. Johnson, **Early Fault-Tolerant Quantum Computing**, *Phys Rev. X QUANTUM* **5** (2024) 020101